Earth and Planetary Science Letters 311 (2011) 225–229

Contents lists available at SciVerse ScienceDirect

Earth and Planetary Science Letters

journal homepage: www.elsevier.com/locate/epsl

Two-stage dissociation in $MgSiO_3$ post-perovskite

Koichiro Umemoto [a,*], Renata M. Wentzcovitch [b]

[a] Department of Geology and Geophysics, University of Minnesota, 3 421 Washington Ave 4 SE, Minneapolis, MN 55455, USA
[b] Minnesota Supercomputing Institute and Department of Chemical Engineering and Materials Science, University of Minnesota, 421 Washington Ave SE, Minneapolis, MN 7 55455, USA

ARTICLE INFO

Article history:
Received 26 May 2011
Received in revised form 8 September 2011
Accepted 21 September 2011
Available online 20 October 2011

Editor: L. Stixrude

Keywords:
pressure-induced phase transition
postperovskite
super-Earth
10 solar giants
first principles

ABSTRACT

The fate of $MgSiO_3$ post-perovskite under TPa pressures is key information for understanding and modeling interiors of super-Earths-type exoplanets and solar giants' cores. Here, we report a dissociation of $MgSiO_3$ post-perovskite into CsCl-type MgO and $P2_1/c$-type $MgSi_2O_5$ at ~0.9 TPa obtained by first principles calculations. $P2_1/c$-type $MgSi_2O_5$ should dissociate further into CsCl-type MgO and Fe_2P-type SiO_2 at ~2.1 TPa. The first dissociation should occur in all solar giants and heavy super-Earths, while the second one should occur only in Jupiter and larger exoplanets. Both dissociations are endothermic and have large negative Clapeyron slopes. If the first dissociation should occur in the middle of a silicate mantle, it could promote mantle layering. We provide essential thermodynamic properties of $P2_1/c$-type $MgSi_2O_5$ for modeling interiors of super-Earths.

1. Introduction

Since the discovery of $MgSiO_3$ post-perovskite (PPV) at conditions similar to those found near the core-mantle boundary (CMB) of the Earth (Murakami et al., 2004; Oganov and Ono, 2004; Tsuchiya et al., 2004), the fate of PPV under further compression has been a puzzling question. The significance of this question has increased greatly after several exoplanets with masses of a few to 10 $M_\oplus$ ($M_\oplus$: Earth mass) were identified (Batalha et al., 2011; Beaulieu et al., 2006; Charbonneau et al., 2009; Leger et al., 2009; Lissauer et al., 2011; Mayor et al., 2009; Queloz et al., 2009; Rivera et al., 2005; Udry et al., 2007). Several of these planets are expected to be Earth-like, i.e., terrestrial, because of their estimated high densities. These exoplanets are frequently referred to as super-Earths. Valencia et al. calculated interior pressure–temperature profiles of super-Earths with masses of 1 to 10 $M_\oplus$ (Valencia et al., 2006). Sotin et al. also calculated them for super-Earths and for ocean exoplanets with 50% H_2O (Sotin et al., 2007). These calculations revealed that pressure and temperature in these exoplanets should be considerably higher than those in Earth, making the fate of $MgSiO_3$ at higher pressures a question of practical relevance for modeling these planets. In this context, $MgSiO_3$ PPV was predicted by first principles to dissociate into CsCl-type MgO and cotunnite-type SiO_2 at ~1 TPa (Umemoto et al., 2006a). This prediction was based on the assumption that $MgSiO_3$ might dissociate into MgO and SiO_2. However, some experiments have recently reported other types of dissociation in ABO_3 perovskites – where A and B are transition-metal atoms – into AO and AB_2O_5 (Okada et al., 2010; Wu et al., 2009). These findings suggested the possibility that $MgSiO_3$ PPV might not dissociate directly into MgO and SiO_2.

In the present paper, we predict the dissociation of $MgSiO_3$ PPV into CsCl-type MgO and $P2_1/c$-type $MgSi_2O_5$. To our knowledge, this $P2_1/c$-type structure has not been identified experimentally in other substances so far. Furthermore, $P2_1/c$-type $MgSi_2O_5$ is found to dissociate into CsCl-type MgO and Fe_2P-type SiO_2 under further compression. We also discuss whether or not the first and the second dissociations may occur in the cores of the solar giantsand in super-Earths. Thermodynamic quantities essential for modeling interiors of super-Earths are provided.

2. Computational method

Calculations were performed using the local-density approximation (LDA) (Ceperley and Alder, 1980; Perdew and Zunger, 1981). All pseudopotentials were generated by Vanderbilt's method (Vanderbilt, 1990). The valence electronic configurations and cutoff radii were the same as used in (Umemoto et al., 2006a). The plane-wave cutoff energy was 400 Ry. We used variable-cell-shape molecular dynamics (Wentzcovitch, 1991; Wentzcovitch et al., 1993) for structural optimization under arbitrary pressure. Dynamical matrices were computed using density functional perturbation theory (Baroni et al., 2001; Giannozzi et al., 1991). We computed the vibrational contribution to the free energies within quasiharmonic approximation (QHA) (Carrier et al., 2008; Wallace, 1972). **k**-point grid for electronic-structure calculations and **q**-point grid for QHA were $(6\times6\times2, 12\times12\times10)$ for $MgSiO_3$ PPV, $(8\times8\times8,$

* Corresponding author. Fax: +1 612 626 7246.
E-mail addresses: umemo001@umn.edu (K. Umemoto), wentz002@umn.edu (R.M. Wentzcovitch).

0012-821X/$ – see front matter © 2011 Elsevier B.V. All rights reserved.
doi:10.1016/j.epsl.2011.09.032

16×16×16) for CsCl-type MgO, (4×4×6, 16×16×16) for Fe_2P-type SiO_2, and (4×2×2, 10×8×10) for $P2_1/c$-type $MgSi_2O_5$.

3. Results and discussion

To investigate the dissociation, we need to know potential high-pressure forms of MgO, SiO_2, and $MgSi_2O_5$. There are no experimental studies for these oxides at extreme dissociation pressures. For MgO, the high-pressure form is assumed to be CsCl-type. The calculated pressure for the NaCl-type-to-CsCl-type transition is 0.53 TPa, consistent with other first-principles calculations (Karki et al., 1997; Mehl et al., 1988; Oganov et al., 2003; Wu et al., 2008). Very recently, the Fe_2P-type phase was predicted to be a post-pyrite phase of SiO_2 beyond 0.69 TPa (Tsuchiya and Tsuchiya, 2011; Wu et al., 2011) at lower temperatures.

To predict the stable phase of $MgSi_2O_5$, we start with the structure of high-pressure $CaGe_2O_5$ (post-titanite) (Nemeth et al., 2007) with space group *Pbam*. There are two types of germanium in this structure, one six-fold and one five-fold coordinated. Germanium octahedra share edges and calcium atoms are eight-fold coordinated in dicapped triangular prisms. Hence, post-titanite and PPV structures have common features, despite having different number of atoms per formula unit. Fig. 1(a) and (b) shows structures of *Pbam*-type $MgSi_2O_5$ optimized at 0 and 1 TPa. Under compression, cation-oxygen connectivity changes clearly; coordination number of Si2 increases from 5 to 8. Pbam-type $MgSi_2O_5$ is dynamically unstable, since there are soft modes with imaginary frequencies at Γ and Y points (Fig. 2). Reoptimizations after applying atomic displacements corresponding to each soft mode reveal that the soft mode at the Γ point leads to the lowest-enthalpy structure (Fig. 1(c)). Across this transformation, only the two-fold screw axis along the a axis and the b glide plane perpendicular to the a axis remain. Then the symmetry is reduced from *Pbam* to its subgroup, $P2_1/b11$. The $P2_1/b11$ setting is not standard. Its symmetrically-equivalent standard setting is $P2_1/c$ (i.e., $P12_1/c1$). Hereafter, we refer to the new phase as $P2_1/c$ $MgSi_2O_5$. Besides this $P2_1/c$ phase, we also considered the structures of P-1-type and $A2/a$-type $CaSi_2O_5$ (Angel, 1997; Angel et al., 1996), *Bbmm*-type $MgTi_2O_5$ (Yang and Hazen, 1998), $C2/c$-type V_3O_5 (Armbruster et al., 2009), and $C2/c$-type $Fe_{1+\delta}Ti_{2-\delta}O_5$ (Wu et al., 2009). Enthalpy calculations clarified that these phases are metastable with respect to the $P2_1/c$ phase (Fig. 3). Therefore, the $P2_1/c$ phase is the most probable candidate form of $MgSi_2O_5$ at high pressures. Structural parameters of the $P2_1/c$ phase at 1 TPa are listed in Table 1. Although the symmetry of this phase is monoclinic, β, the angle between a and c axes, is very close to 90°. Thus, the monoclinic distortion from the *Pbam* orthorhombic cell is very small.

Now we have the necessary ingredients to discuss the dissociation of $MgSiO_3$ PPV. Fig. 4 shows $MgSiO_3$ PPV should dissociate into CsCl-type MgO and $P2_1/c$-type $MgSi_2O_5$ at 0.90 TPa. This dissociation pressure is 0.21 TPa lower than that of the direct dissociation of $MgSiO_3$ into MgO and SiO_2. It is also seen that $P2_1/c$-type $MgSi_2O_5$ must dissociate into CsCl-type MgO and Fe_2P-type SiO_2 at 2.10 TPa. Silicon coordination numbers increase across both dissociations: 6 in $MgSiO_3$ PPV, 7 and 8 in $P2_1/c$-type $MgSi_2O_5$, and 9 in Fe_2P-type SiO_2. Correspondingly, volume reduces by 2.3% (0.5%) across the first (second) dissociation. We did not find a transition to any post-PPV crystalline phase with $MgSiO_3$ formula unit. The U_2S_3-type phase, a potential post-PPV candidate (Umemoto and Wentzcovitch, 2006, 2008), always has higher enthalpy than those of aggregated dissociation products. Dissociation pressures by PBE-type generalized-gradient approximation (GGA) (Perdew et al., 1981) are 0.89 and 2.04 TPa for the first and the second dissociation. They are slightly smaller than LDA results, which contrasts with the usual tendency. The differences between LDA and GGA are small: about 1% (3%) for the first (second) dissociation.

Fig. 5 shows the dissociation boundaries of $MgSiO_3$ calculated using the QHA. In the solar giants, $MgSiO_3$ PPV should not survive. In Saturn, Uranus, and Neptune, MgO and $MgSi_2O_5$ are expected to occur in their dense cores. In Jupiter, $MgSi_2O_5$ should be dissociated into MgO and SiO_2. For super-Earths and ocean exoplanets with 1–10 $M_\oplus$, internal pressure and temperature have been estimated (Sotin et al., 2007; Valencia et al., 2006). According to these estimations and dissociation phase boundaries, $MgSiO_3$ PPV should survive in super-Earths with masses smaller than ~7$M_\oplus$. The first dissociation should occur only

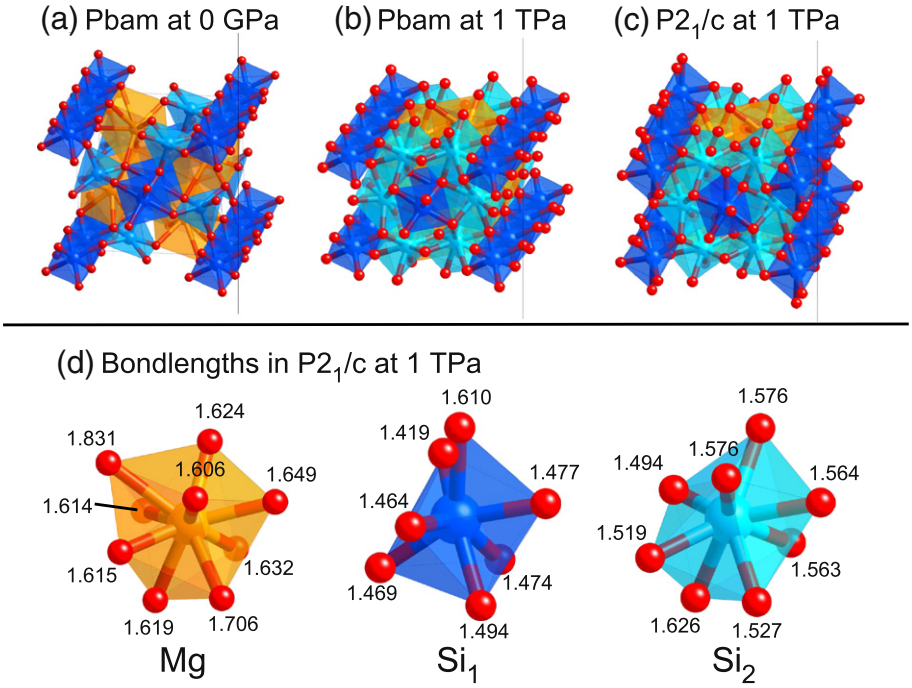

Fig. 1. Crystal structures of (a) *Pbam*-type $MgSi_2O_5$ at 0 GPa, (b) at 1 TPa, and (c) $P2_1/c$-type at 1 TPa. (d) Bonglengths (Å) between cations and oxygens in $P2_1/c$-type $MgSi_2O_5$. Yellow, blue, light blue, and red spheres denote Mg, Si_1, Si_2, and O atoms.

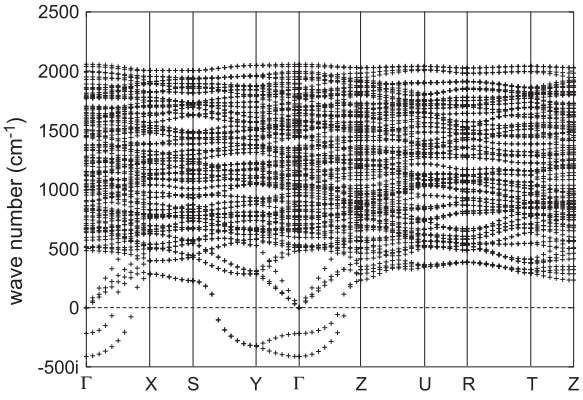

Fig. 2. Phonon dispersion of *Pbam*-type $MgSi_2O_5$ at 1 TPa.

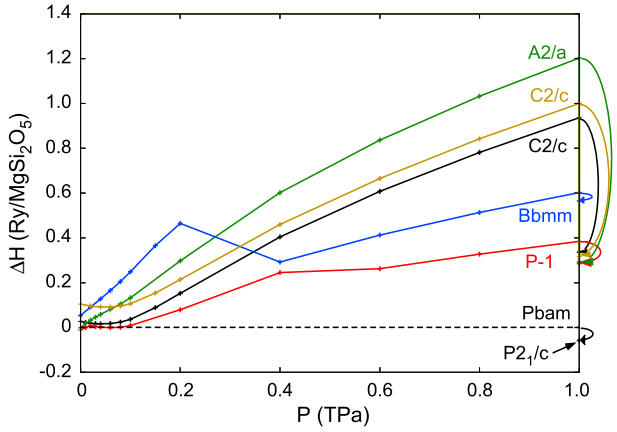

Fig. 3. Relative enthalpies of several candidates of $MgSi_2O_5$ with respect to the *Pbam*-type phase. All candidates are dynamically unstable at 1 TPa. Arrows denote enthalpy reduction by reoptimization after applying atomic displacements corresponding to soft modes.

in larger super-Earths, but not the second one. In ocean exoplanets, the first dissociation may occur when their masses are larger than ~$8M_\oplus$. Therefore, $MgSiO_3$ PPV should dissociate into MgO and $MgSi_2O_5$ in GJ876d (Rivera et al., 2005) but should not in CoRoT-7b (Leger et al., 2009; Queloz et al., 2009), GJ1214b (Charbonneau et al., 2009), Kepler-10b (Batalha et al., 2011), nor Kepler-11b (Lissauer et al., 2011). Thermodynamic properties are fundamental for modeling the internal state of these planets and they are provided up to 6000 K in Table 2.

Both dissociations are endothermic, because their phase boundaries have negative Clapeyron slopes: −12 (−31) MPa/K at 5000 K and −20 (−38) MPa/K at 10,000 K in the first (second) dissociation. These can be explained by changes in vibrational density of states.

Table 1
Structural parameters of $P2_1/c$-type $MgSi_2O_5$. Wyckoff positions of all atoms are *4e*: $(x,y,z),(-x,y+1/2,-z+1/2),(-x,-y,-z)$, and $(x,-y+1/2,z+1/2)$.

(a,b,c) (Å)	(4.429, 4.031, 6.179)
β (°)	89.68
Mg	(0.5054, 0.6686, 0.0638)
Si_1	(0.2580, 0.0699, 0.9916)
Si_2	(0.9966, 0.0498, 0.6757)
O_1	(0.2411, 0.1748, 0.2203)
O_2	(0.2351, 0.8453, 0.8052)
O_3	(0.2294, 0.0322, 0.5002)
O_4	(0.5431, 0.1901, 0.9209)
O_5	(0.0393, 0.6735, 0.5855)

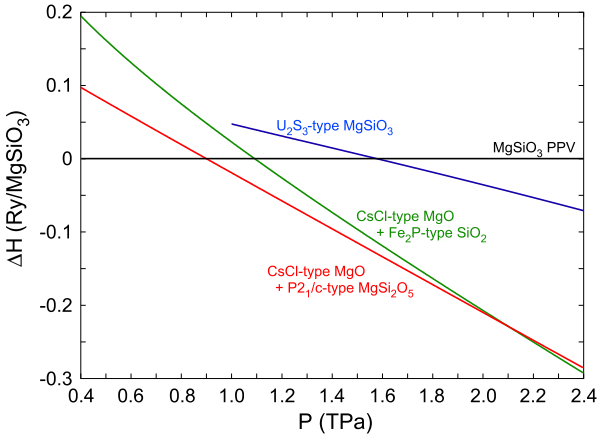

Fig. 4. Relative enthalpies of aggregation of CsCl-type MgO and $P2_1/c$-type $MgSi_2O_5$, CsCl-type MgO and Fe_2P-type SiO_2, and U_2S_3-type $MgSiO_3$ with respect to $MgSiO_3$ PPV.

Across both dissociations, while volume decreases Si–O bond lengths and Si coordination numbers increase. Longer bonds lead to smaller optic phonon frequencies and larger vibrational entropy. Therefore, aggregated dissociation products have larger stability fields at higher temperatures, resulting in a negative Clapeyron slope (Navrotsky, 1980). An endothermic phase transition can affect mantle dynamics in exoplanets with silicate mantle. Dissociations with large negative Clapeyron slopes in the middle of a silicate mantle can in principle promote layering (Christensen and Yuen, 1985; Peltier and Solheim, 1992; Tackley, 1995). However, other factors, such as pressure and temperature dependent properties, might conspire against layered convection. Change of viscosity across the dissociation could also affect significantly mantle dynamics in super-Earths (Karato, 2011; van den Berg et al., 2010). Present results are just a starting point for considering these effects.

The two-stage dissociation of $MgSiO_3$ PPV reported here may also help to solve open questions concerning the high-pressure behavior of ABX_3 compounds. The dissociation of $NaMgF_3$ PPV, a low-pressure analog of $MgSiO_3$ was predicted to happen at ~40 GPa (Umemoto et al., 2006b), but it has not been observed experimentally. Moreover, there are inconsistencies between experiments; while (Martin

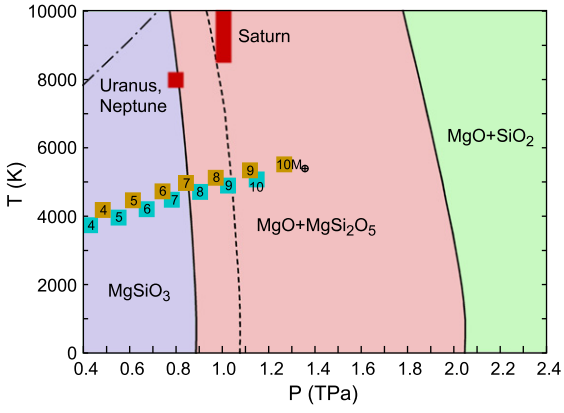

Fig. 5. Phase diagram showing the two-stage dissociation of $MgSiO_3$ PPV. Red spots denote estimated pressure–temperature conditions at core-envelope boundaries in the solar giants (Jupiter's condition, ~4 TPa and ~15,000? 20,000 K, is not shown here) (Guillot, 2004). Brown and light blue squares represent pressure–temperature conditions at CMB in terrestrial and ocean exoplanets (Sotin et al., 2007). Numbers in squares indicate the planet mass in units of Earth mass ($M_\oplus$).Dashed phase boundary is the metastable boundary of the direct dissociation of $MgSiO_3$ into MgO and SiO_2. A dot-dashed line denotes the limit of validity of the QHA (Tsuchiya et al., 2005).

Table 2
Thermodynamic properties of $P2_1/c$-type $MgSi_2O_5$: density (ρ), thermal expansivity (α), isothermal bulk modulus (K_T), adiabatic bulk modulus (K_S), constant-volume heat capacity (C_V), constant-pressure heat capacity (C_P), and Grüneisen parameter (γ). Values for the other phases will be available online at http://www.vlab.msi.umn.edu.

P (TPa)	ρ (g/cm^3)	α (10^{-5}/K)	K_T (TPa)	K_S (TPa)	C_V (J/mol/K)	C_P (J/mol/K)	γ
1000 K							
0.4	7.3418	0.5630	1.5000	1.5092	170.5582	171.5977	1.0827
0.6	8.2219	0.4354	2.0594	2.0689	164.1819	164.9443	1.0664
0.8	8.9616	0.3571	2.6027	2.6125	158.5342	159.1288	1.0503
1.0	9.6104	0.3033	3.1350	3.1448	153.4502	153.9319	1.0350
1.2	10.1943	0.2637	3.6587	3.6686	148.8213	149.2219	1.0209
1.4	10.7290	0.2332	4.1756	4.1854	144.5712	144.9111	1.0080
1.6	11.2249	0.2090	4.6868	4.6965	140.6441	140.9371	0.9963
1.8	11.6890	0.1894	5.1931	5.2028	136.9974	137.2533	0.9860
2.0	12.1267	0.1731	5.6951	5.7047	133.5976	133.8236	0.9770
2.2	12.5419	0.1595	6.1933	6.2028	130.4179	130.6194	0.9693
2000 K							
0.4	7.2974	0.6306	1.4812	1.5012	191.6985	194.2906	1.0721
0.6	8.1826	0.5030	2.0390	2.0607	189.7636	191.7880	1.0604
0.8	8.9258	0.4241	2.5811	2.6041	187.9332	189.6029	1.0476
1.0	9.5772	0.3693	3.1124	3.1362	186.2020	187.6253	1.0348
1.2	10.1632	0.3287	3.6353	3.6597	184.5595	185.8004	1.0228
1.4	10.6997	0.2972	4.1515	4.1765	182.9956	184.0959	1.0116
1.6	11.1970	0.2719	4.6622	4.6876	181.5019	182.4901	1.0013
1.8	11.6624	0.2511	5.1680	5.1938	180.0710	180.9681	0.9920
2.0	12.1011	0.2337	5.6697	5.6958	178.6968	179.5184	0.9837
2.2	12.5173	0.2189	6.1677	6.1941	177.3742	178.1323	0.9763
3000 K							
0.4	7.2508	0.6477	1.4628	1.4933	196.0335	200.1094	1.0701
0.6	8.1407	0.5195	2.0190	2.0523	195.1422	198.3657	1.0600
0.8	8.8872	0.4403	2.5598	2.5952	194.2889	196.9783	1.0479
1.0	9.5410	0.3854	3.0899	3.1270	193.4736	195.7906	1.0357
1.2	10.1289	0.3447	3.6120	3.6502	192.6930	194.7333	1.0240
1.4	10.6669	0.3130	4.1274	4.1667	191.9435	193.7695	1.0131
1.6	11.1655	0.2876	4.6374	4.6776	191.2219	192.8767	1.0029
1.8	11.6320	0.2667	5.1428	5.1837	190.5254	192.0405	0.9937
2.0	12.0718	0.2492	5.6441	5.6857	189.8517	191.2506	0.9854
2.2	12.4887	0.2344	6.1417	6.1840	189.1988	190.4997	0.9780
4000 K							
0.4	7.2037	0.6563	1.4448	1.4854	197.5758	203.1239	1.0696
0.6	8.0982	0.5271	1.9993	2.0440	197.0693	201.4745	1.0602
0.8	8.8478	0.4474	2.5387	2.5864	196.5819	200.2710	1.0485
1.0	9.5039	0.3923	3.0678	3.1177	196.1143	199.3039	1.0365
1.2	10.0937	0.3513	3.5888	3.6405	195.6650	198.4833	1.0249
1.4	10.6332	0.3195	4.1035	4.1567	195.2322	197.7626	1.0140
1.6	11.1331	0.2940	4.6129	4.6674	194.8142	197.1145	1.0040
1.8	11.6006	0.2731	5.1177	5.1733	194.4097	196.5219	0.9948
2.0	12.0413	0.2555	5.6185	5.6752	194.0172	195.9731	0.9864
2.2	12.4591	0.2405	6.1158	6.1734	193.6359	195.4598	0.9790
5000 K							
0.4	7.1563	0.6625	1.4270	1.4776	198.2912	205.3160	1.0695
0.6	8.0554	0.5321	1.9798	2.0357	197.9662	203.5521	1.0606
0.8	8.8081	0.4518	2.5179	2.5776	197.6524	202.3372	1.0491
1.0	9.4665	0.3963	3.0458	3.1084	197.3507	201.4071	1.0373
1.2	10.0581	0.3551	3.5659	3.6308	197.0603	200.6495	1.0258
1.4	10.5991	0.3232	4.0798	4.1467	196.7800	200.0069	1.0149
1.6	11.1002	0.2975	4.5885	4.6571	196.5089	199.4462	1.0048
1.8	11.5688	0.2765	5.0927	5.1628	196.2461	198.9467	0.9956
2.0	12.0104	0.2588	5.5931	5.6645	195.9908	198.4945	0.9872
2.2	12.4289	0.2438	6.0900	6.1627	195.7424	198.0800	0.9797
6000 K							
0.4	7.1089	0.6676	1.4095	1.4699	198.6789	207.1911	1.0696
0.6	8.0125	0.5360	1.9605	2.0274	198.4533	205.2252	1.0610
0.8	8.7682	0.4551	2.4972	2.5688	198.2350	203.9178	1.0498
1.0	9.4289	0.3992	3.0240	3.0992	198.0247	202.9483	1.0380
1.2	10.0223	0.3578	3.5431	3.6212	197.8220	202.1813	1.0265
1.4	10.5647	0.3256	4.0562	4.1367	197.6261	201.5478	1.0157
1.6	11.0671	0.2999	4.5642	4.6468	197.4365	201.0084	1.0056
1.8	11.5367	0.2787	5.0679	5.1523	197.2526	200.5384	0.9963
2.0	11.9792	0.2609	5.5678	5.6539	197.0738	200.1217	0.9879
2.2	12.3985	0.2458	6.0643	6.1520	196.8997	199.7469	0.9804

et al., (2006) reported a post-PPV transition to a "N-phase", whose structure has not been identified yet, other experiments showed that the PPV phase remained stable (Grocholski et al., 2010; Hustoft et al., 2008). The new dissociation found here might shed light on this inconsistency. Very recently, $MnTiO_3$ perovskite was reported to dissociate into MnO and $MnTi_2O_5$ (Okada et al., 2010). Although $MnTi_2O_5$ was expected to be orthorhombic, its detailed structure has not been identified yet. As showed here, $P2_1/c$-type $MgSi_2O_5$ has a small monoclinic distortionfrom the orthorhombic cell. We expect the structure of $P2_1/c$-type $MgSi_2O_5$ to be closely related to that of $MnTi_2O_5$.

Acknowledgments

We would like to thank Professor D. A. Yuen for fruitful discussions. Calculations have been done using the Quantum-ESPRESSO package (Giannozzi et al., 2009) and VLab software (da Silveira et al., 2008). Research was supported by NSF grants EAR-1047629. Computations were performed at the Minnesota Supercomputing Institute and at the Laboratory for Computational Science and Engineering at the University of Minnesota.

References

Angel, R.J., Ross, N.L., Seifert, F., Fliervoet, T.F., 1996. Structural characterization of pentacoordinate silicon in a calcium silicate. Nature 384, 441–444.
Angel, R.J., 1997. Transformation of fivefold-coordinated silicon to octahedral silicon in calcium silicate, $CaSi_2O_5$. Am. Mineral. 82, 836–839.
Armbruster, T., Galuskin, E.V., Reznitsky, L.Z., Sklyarov, E.V., 2009. X-ray structural investigation of the oxyvanite (V_3O_5)-berdesinskiite (V_2TiO_5) series: V^{4+} substituting for octahedrally coordinated Ti^{4+}. Eur. J. Mineral. 21, 885–891.
Baroni, S., de Gironcoli, S., Dal Corso, A., Giannozzi, P., 2001. Phonons and related crystal properties from density-functional perturbation theory. Rev. Mod. Phys. 73, 515–562.
Batalha, N.M., et al., 2011. Kepler's First Rocky Planet: Kepler-10b. Astrophys. J. 729, 27.
Beaulieu, J.P., et al., 2006. Discovery of a cool planet of 5.5 Earth masses through gravitational microlensing. Nature 439, 437–440.
Carrier, P., Justo, J.F., Wentzcovitch, R.M., 2008. Quasiharmonic elastic constants corrected for deviatoric thermal stresses. Phys. Rev. B 78, 144302.
Ceperley, D.M., Alder, B.J., 1980. Ground state of the electron gas by a stochastic method. Phys. Rev. Lett. 45, 566–569.
Charbonneau, D., et al., 2009. A super-Earth transiting a nearby low-mass star. Nature 462, 891.
Christensen, U.R., Yuen, D.A., 1985. Layered convection induced by phase transitions. J. Geophys. Res. 90, 10291–10300.
da Silveira, P.R.C., da Silva, C.R.S., Wentzcovitch, R.M., 2008. Metadata management for distributed first principles calculations in *VLab*–A collaborative cyberinfrastructure for materials computation. Comput. Phys. Commun. 178, 186–198.
Giannozzi, P., de Gironcoli, S., Pavone, P., Baroni, S., 1991. Ab initio calculation of phonon dispersions in semiconductors. Phys. Rev. B 43, 7231–7242.
Giannozzi, P., et al., 2009. QUANTUM ESPRESSO: a modular and open-source software project for quantum simulations of materials. J. Phys. Condens. Matter 21, 395502 http://www.quantum-espresso.org.
Grocholski, B., Shim, S.H., Prakapenka, V.B., 2010. Stability of the $MgSiO_3$ analog $NaMgF_3$ and its implication for mantle structure in super-Earths. Geophys. Res. Lett. 37, L14204.
Guillot, T., 2004. Probing the Giant Planets. Phys. Today 57, 63.
Hustoft, J., Catalli, K., Shim, S.H., Kubo, A., Prakapenka, V.B., Kuntz, M., 2008. Equation of state of $NaMgF_3$ postperovskite: implication for the seismic velocity changes in the D″ region. Geophys. Res. Lett. 35, L10309.
Karato, S., 2011. Rheological structure of the mantle of a super-Earth: some insights from mineral physics. Icarus 212, 14–23.
Karki, B.B., Stixrude, L., Clark, S.J., Warren, M.C., Ackland, G.J., Crain, J., 1997. Structure and elasticity of MgO at high pressure. Am. Mineral. 82, 51–60.
Leger, A., et al., 2009. Transiting exoplanets from the CoRoT space mission VIII. CoRoT-7b: the first super-Earth with measured radius. Astron. Astrophys. 506, 287–302.
Lissauer, J.J., et al., 2011. A closely packed system of low-mass, low-density planets transiting Kepler-11. Nature 470, 53–58.
Martin, C.D., Crichton, W.A., Liu, H., Prakapenka, V., Chen, J., Parise, J.B., 2006. Phase transitions and compressibility of $NaMgF_3$ (Neighborite) in perovskite- and post-perovskite-related structures. Geophys. Res. Lett. 33, L11305.
Mayor, M., Udry, S., Lovis, C., Pepe, F., Queloz, D., Benz, W., Bertaux, J.L., Bouchy, F., Mordasini, C., Segransan, D., 2009. The HARPS search for southern extra-solar planets XIII. A planetary system with 3 super-Earths (4.2, 6.9, and 9.2 $M_\oplus$). Astron. Astrophys. 493, 639–644.
Mehl, M.J., Cohen, R.E., Krakauer, H., 1988. Linearized augmented plane wave electronic structure calculations for MgO and CaO. J. Geophys. Res. 93, B8009–B8022.

Murakami, M., Hirose, K., Kawamura, K., Sata, N., Ohishi, Y., 2004. Post-perovskite phase transition in $MgSiO_3$. Science 304, 855–858.
Navrotsky, A., 1980. Lower mantle phase transitions may generally have negative pressure-temperature slopes. Geophys. Res. Lett. 7, 709–711.
Nemeth, P., Leinenweber, K., Groy, T.L., Buseck, P.R., 2007. A new high-pressure $CaGe_2O_5$ polymorph with 5- and 6-coordinated germanium. Am. Mineral. 92, 441–443.
Oganov, A.R., Gillan, M.J., Price, G.D., 2003. Ab initio lattice dynamics and structural stability of MgO. J. Chem. Phys. 118, 10174–10182.
Oganov, A.R., Ono, S., 2004. Theoretical and experimental evidence for a post-perovskite phase of $MgSiO_3$ in Earth's D″ layer. Nature 430, 445–448.
Okada, T., Yagi, T., Nishio-Hamane, D., 2010. High-pressure phase behavior of $MnTiO_3$: decomposition of perovskite into MnO and $MnTi_2O_5$. Phys. Chem. Miner. 38, 251–258.
Peltier, W.R., Solheim, L.P., 1992. Mantle phase transitions and layered chaotic convection. Geophys. Res. Lett. 19, 321–324.
Perdew, J.P., Zunger, A., 1981. Self-interaction correction to density-functional approximations for many-electron systems. Phys. Rev. B 23, 5048–5079.
Perdew, J.P., Burke, K., Ernzerhof, M., 1981. Generalized gradient approximation made simple. Phys. Rev. Lett. 77, 3865–3868.
Queloz, D., et al., 2009. The CoRoT-7 planetary system: two orbiting super-Earths. Astron. Astrophys. 506, 303–319.
Rivera, E.J., Lissauer, J.J., Butler, R.P., Marcy, G.W., Vogt, S.S., Fischer, D.A., Brown, T.M., Laughlin, G., Henry, G.W., 2005. A $\sim 7.5M_{\oplus}$ Planet Orbiting the Nearby Star, GJ 876. Astrophys. J. 634, 625–640.
Sotin, C., Grasset, O., Mocquet, A., 2007. Mass-radius for extrasolar Earth-like planets and ocean planets. Icarus 191, 337–351.
Tackley, P.J., 1995. On the penetration of an endothermic phase transition by upwellings and downwellings. J. Geophys. Res. 100, 15477–15488.
Tsuchiya, T., Tsuchiya, J., Umemoto, K., Wentzcovitch, R.M., 2004. Phase transition in $MgSiO_3$ perovskite in the earth's lower mantle. Earth Planet. Sci. Lett. 224, 241–248.
Tsuchiya, J., Tsuchiya, T., Wentzcovitch, R.M., 2005. Vibrational and thermodynamic properties of $MgSiO_3$ post-perovskite. J. Geophys. Res. 110 (B2), B02204.
Tsuchiya, T., Tsuchiya, J., 2011. Prediction of a hexagonal SiO_2 phase affecting stabilities of $MgSiO_3$ and $CaSiO_3$ at multimegabar pressures. Proc. Natl. Acad. Sci. 108, 1252–1255.
Udry, S., Bonfils, X., Delfosse, X., Forveille, T., Mayor, M., Perrier, C., Bouchy, F., Lovis, C., Pepe, F., Queloz, D., Bertaux, J.L., 2007. The HARPS search for southern extra-solar planets XI. Super-Earths (5 and 8 $M_{\oplus}$) in a 3-planet system. Astron. Astrophys. 469, L43–L47.
Umemoto, K., Wentzcovitch, R.M., Allen, P.B., 2006a. Dissociation of $MgSiO_3$ in the cores of gas giants and terrestrial exoplanets. Science 311, 983–986.
Umemoto, K., Wentzcovitch, R.M., Weidner, D.J., Parise, J.B., 2006b. $NaMgF_3$: A low-pressure analog of $MgSiO_3$. Geophys. Res. Lett. 33, L15304.
Umemoto, K., Wentzcovitch, R.M., 2006. Potential ultrahigh pressure polymorphs of ABX_3-type compounds. Phys. Rev. B 224105.
Umemoto, K., Wentzcovitch, R.M., 2008. Prediction of an U_2S_3-type polymorph of Al_2O_3 at 3.7 Mbar. Proc. Natl. Acad. Sci. 6526–6530.
Valencia, D., O'Connell, R.J., Sasselov, D., 2006. Internal structure of massive terrestrial planets. Icarus 181, 545–554.
van den Berg, A.P., Yuen, D.A., Beebe, G.L., Christiansen, M.D., 2010. The dynamical impact of electronic thermal conductivity on deep mantle convection of exosolar planets. Phys. Earth Planet. Inter. 178, 136–154.
Vanderbilt, D., 1990. Soft self-consistent pseudopotentials in a generalized eigenvalue formalism. Phys. Rev. B 41, R7892–R7895.
Wallace, D., 1972. Thermodynamics of Crystals. Wiley, New York.
Wentzcovitch, R.M., 1991. Invariant molecular-dynamics approach to structural phase transitions. Phys. Rev. B 44, 2358–2361.
Wentzcovitch, R.M., Martins, J.L., Price, G.D., 1993. *Ab initio* molecular dynamics with variable cell shape: application to $MgSiO_3$. Phys. Rev. Lett. 70, 3947–3950.
Wu, Z., Wentzcovitch, R.M., Umemoto, K., Li, B., Hirose, K., Zheng, J.C., 2008. Pressure–volume–temperature relations in MgO: an ultrahigh pressure–temperature scale for planetary sciences applications. J. Geophys. Res. 113, B06204.
Wu, X., Steinle-Neumann, G., Narygina, O., Kantor, I., McCammon, C., Prakapenka, V., Swamy, V., Dubrovinsky, L., 2009. High-pressure behavior of perovskite: $FeTiO_3$ dissociation into $(Fe_{1-\delta}, Ti_{\delta})O$ and $Fe_{1+\delta}Ti_{2-\delta}O_5$. Phys. Rev. Lett. 103, 065503.
Wu, S., Umemoto, K., Ji, M., Wang, C.Z., Ho, K.M., Wentzcovitch, R.M., 2011. Identification of post-pyrite phase transitions in SiO_2 by a genetic algorithm. Phys. Rev. B 83, 184102.
Yang, H., Hazen, R.M., 1998. Crystal chemistry of cation order–disorder in pseudobrookite-type $MgTi_2O_5$. J. Solid State Chem. 138, 238–244.